Soils and Foundations 2015;55(6):1474–1486

HOSTED BY

ELSEVIER

CrossMark

The Japanese Geotechnical Society

Soils and Foundations

www.sciencedirect.com

journal homepage: www.elsevier.com/locate/sandf

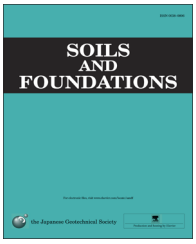

Compaction control and related stress–strain behaviour of off-shore land reclamations with calcareous sands

P.O. Van Impe[a,b,*], W.F. Van Impe[a,b], A. Manzotti[b], P. Mengé[c], M. Van den Broeck[c], K. Vinck[c]

[a]*Ghent University, Laboratory of Geotechnics, Technologiepark 9, 9052 Zwijnaarde, Belgium*
[b]*AGE bvba Geotechnical Consultants, Rooseveltlaan 2, 9420 Erpe-Mere, Belgium*
[c]*DEME NV, Scheldedijk 30, 2070 Zwijndrecht, Belgium*

Received 19 September 2014; received in revised form 12 June 2015; accepted 25 July 2015
Available online 23 December 2015

Abstract

When constructing off-shore land reclamations, one aims to ensure that the final soil mass fulfills certain minimal criteria related to shear strength, stiffness and resistance against liquefaction. In general, these characteristics improve with increasing density of the soil mass, which means that the above criteria are usually condensed into a single one: 'adequate densification'.

Quality control of reclamation constructions therefore focuses on the latter. Technical requirements are written based on one single parameter: the relative density D_r. On the site, this parameter is commonly determined indirectly using correlations with the cone penetration resistance q_c, making the CPT the main tool for quality control.

The paper presents data gathered during the design and construction of an off-shore land reclamation using calcareous sands. For this specific project, density control had to be done through the use of CPT.

Calibration chamber tests were performed to establish the CPT q_c–D_r correlation for the specific soil material. This correlation was used to analyse CPT results during construction of the site in order to determine the quality of compaction.

In a further stage, an elaborate laboratory study was performed to establish additional correlations between soil parameters and the stress–strain parameters. Furthermore, seismic CPT tests were executed on the site to test the relevance of the laboratory correlations and the 'relative density approach' in general.

It is shown that off-shore land reclamations have a very erratic stress-history, due to the different processes of depositing the soil material and the various densification methods. This stress-history is of great importance in the stress–strain behaviour of the site. Results also suggest that the CPT does not provide enough data to reliably predict soil stiffness when dealing with crushable materials. Specifically, in situ measurements show that there is no direct correlation between the small strain shear modulus G_0 and q_c.

Keywords: Reclamation; Compaction control; Calibration chamber testing; SCPT; Calcareous sand; Resonant column; Bender element

*Principal corresponding author at : AGE bvba, Rooseveltlaan 2, 9420 Erpe-Mere, Belgium.
E-mail addresses: peter.vanimpe@age-be.net (P.O. Van Impe), william.vanimpe@age-be.net (W.F. Van Impe), alice.manzotti@age-be.net (A. Manzotti), menge.patrick@deme.be (P. Mengé), van.den.broeck.marc@deme.be (M. Van den Broeck), vinck.ken@deme.be (K. Vinck).
URL: http://www.AGE-be.net (P.O. Van Impe).
Peer review under responsibility of under Japanese Geotechnical Society

http://dx.doi.org/10.1016/j.sandf.2015.10.012

1. Introduction

1.1. Land reclamation quality control

In the philosophy of reclamation quality control, the future stress–strain behaviour of the site is correlated to the density of the fill. Quality control is linked to 'adequate densification', which should guarantee that certain minimal requirements related to the soil behaviour (shear strength, stiffness or cyclic resistance ratio) will be obtained.

This concept is translated into technical requirements using parameters like relative density D_r or maximum dry density (MDD).

Densities are then determined on site either directly (in situ dry density measurement by e.g. the sand replacement method) or indirectly, based on correlations between density and the cone penetration resistance q_c.

During construction of the site, the CPT will be used as a control method to indicate areas where additional densification is required.

1.2. Relevance of using the q_c–D_r approach in compaction control

Authors believe there are ample reasons why the current approach does not reflect the 'quality' of a reclamation.

Firstly, the method depends fully on relative density D_r, which is an extremely unreliable parameter. It is a calculated value depending on particle density, bulk density, minimum and maximum density. Especially the latter are notoriously difficult to pin down as they depend strongly on the method with which they are determined. Moreover, each small error in the measurement of the above parameters has a larger than proportional effect on the final value of D_r.

Especially for crushable sands, this becomes problematic. The measured maximum density is only relevant as long as the sample does not crush. As soon as crushing starts taking place, we are in effect dealing with a different material. This should rule out the use of the proctor compaction to determine the maximum density, although it is the prescribed method in many tender documents.

Some other specific problems with dealing with crushable sands did become common knowledge over the past decade. As it has been shown for many years, the typical correlations between q_c and D_r are no longer valid, as significantly lower q_c values are developed in these sands as compared to silica sands under similar conditions. However, rather than abandon this approach, correction factors have been applied, based on the so-called 'shell-factor'. The shell-factor would be the ratio of the cone penetration resistance (at a certain stress level) for a crushable material and that for a reference (silica) material, and is therefore only relevant for the comparison between these two specific soil materials.

Unfortunately, in practice, this correction method has started a life of its own, losing on the way all connection to reality. It has come to the point where a value of the shell-factor is a result of a negotiation between two opposing forces: the contractor (aiming for the highest value, which would reduce the critical cone resistance limit and therefore the amount of compaction) and the owner or engineering office (aiming at the lowest value in order to force the contractor to perform the highest level of compaction).

Beside the problems on how to determine the compaction quality through CPT, one should question the general principle that – in these soils – adequate soil conditions are reflected by the relative density D_r:

- In many cases, what is assumed to be 'adequate' is not even specified. Technical requirements for a reclamation site rarely specify actual parameters relevant to the stress–strain behaviour.
- The value of the minimum relative density which guarantees 'adequate' soil behaviour is based on general correlations proposed in literature. But if we use – in the case of a calcareous soil – a correction factor to take into account the effect of crushing on the correlation with the cone resistance q_c, why do we still expect the others to be relevant? It has been shown again and again that the cyclic resistance ratio can be far greater in the case of calcareous sands, due to their irregular grain shape (LaVielle, 2008; Pando et al., 2012; Brandes, 2011).
- The effect of crushing is not taken into account, although crushing is inevitable when large compaction efforts are required. One could question if the effect of crushing itself does not negatively alter the soil behaviour, in a way that it compensates the beneficial effect of the increased density, i.e., should we fear 'over-compaction'?

1.3. Present research

The project presented in this paper was an off-shore land reclamation, consisting of two separate islands, located in the Persian Gulf. Typically for this region, the main soil material was a calcareous sand of biogenic origin (shells and coral).

Technical requirements stated that the CPT should be used to establish the degree of densification of the hydraulic fill (through q_c–D_r correlation, according to literature), combined with in situ dry density tests on the layers above the water table. Densification of the hydraulic fill was to be done by vibrocompaction, until values of relative density D_r were above 61% (equivalent to 90% MDD).

During this project, two research campaigns have been organized.

The main dredging contractor chose not to work with the so-called 'shell-factor' approach but instead – with the approval of the site owner and its engineer – organized extensive laboratory calibration chamber testing to obtain the actual relevant q_c–D_r correlation for the site material. As this was still at the very early stages of the project, calibration chamber tests were performed on materials coming from the two main borrow areas.

The second testing campaign was organized in order to check the validity of the q_c–D_r approach – specifically looking at the in situ soil stiffness – and to obtain data which could allow alternative quality control methods. This campaign

consisted of an extensive series of laboratory tests (TX with local strain measurement, resonant column, and bender element) in order to determine the basic stress–strain behaviour of the site material. Additionally, a series of 43 seismic cone penetration tests were performed, providing both cone penetration resistance and small strain shear stiffness along the depth of the reclamation.

2. Index properties of the reclamation material

Samples from the borrow areas are indicated as BAE (borrow area east) and BAW (borrow area west) further in the text.

The material of the second campaign was taken from one island, as soon as it surfaced. This material will be denoted as S1 in this paper.

All materials were analysed to determine standard reference parameters: grain size distribution, carbonate content and index densities. Fig. 1 shows the results of the sieving. As one can notice, there was a significant difference on the particle size distribution of the sands from the borrow areas (BAW and BAE). The material S1 (from the actual reclamation site) was quite close to the material BAW.

As a reference, we compare the particle size distribution (PSD) with other sands typically used in research. Quiou sand (Pallara et al., 1998) is very similar to S1 and BAW. As a silica sand, we can compare these with Ticino (Fioravante, 2000), which has a similar D50, but is more uniform. BAE sand is very close to Dogs Bay sand (Hyodo et al., 1998). These could be compared to Toyoura (Pallara et al., 1998), which again has a similar D50 but is also more uniform.

Table 1 gives an overview of the relevant data on index densities and carbonate content of these materials. As we are dealing with sand particles of a very irregular shape, we obtain values of the minimum and maximum void ratio which are well beyond the typical range for silica sands. Fig. 2 shows the typical form of the biogenic material. Although the materials BAW and BAE have significantly different grain size distributions, they both are essentially identical when it comes to grain morphology, as both have the same geological origin (both sites are situated quite close to each other).

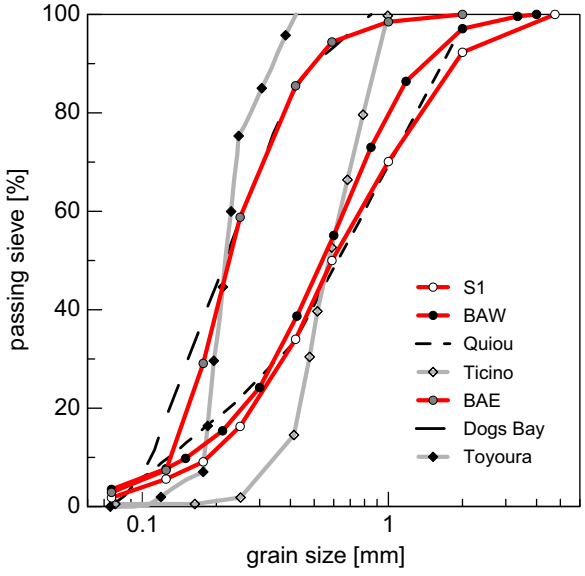

Fig. 1. Grain size distribution of the BAE/BAW/S1 sands and other relevant materials.

Table 1
Overview of sand characteristics.

Sand	G_s (–)	D_{50} (mm)	$CaCO_3$ (%)	e_{max} (–)	e_{min} (–)
S1	2.84	0.59	95	1.278	0.741
BAE	2.84	0.23	93	1.551	0.979
BAW	2.84	0.57	98	1.392	0.843
Dogs Bay	2.75	0.24	87–92	1.83	0.98
Quiou	2.716	0.71	77	1.281	0.831
Kenya sand	2.785	0.13	97	1.776	1.282
Cabo Rojo	2.86	0.38	92.8	1.71	1.34
Toyoura	2.645	0.16		0.977	0.605
Ticino	2.69	0.55		0.934	0.582
Mol	2.65	0.195		0.918	0.585

It can be seen that the S1, BAW and Quiou sands – which have very similar grain size distribution curves – have values of e_{min} and e_{max} which are also fairly similar. Nevertheless, these 'close' values still lead to significant differences in calculated values of the relative density D_r. For example, a void ratio of 1 would be equivalent to a D_r value of 52% in case of the S1 sand, but nearly 72% for BAW and 62% for Quiou sand.

On the other hand, Dogs Bay and BAE – which have almost identical PSDs – have an almost identical maximum high density – i.e., similar value of e_{min} – but a significantly different value of e_{max} (low density). Is this due to particle shape and mineralogy or is it simply due to a different testing method? This complicates a comparison of research data from literature.

Another example to illustrate the sensitivity of the critical parameters of minimum and maximum density is shown in Table 2. We see here a comparison of the values of maximum and minimum density for the same sand, obtained at three different laboratories. We have the obvious variations due to variability in the material itself (batch 1 and batch 2, 2 subsamples of the large sample taken at the borrow area) and the testing method (lab 1 used method C for minimum density). Some variations may be attributed to the accuracy of the lab: lab 1 is a local commercial laboratory while labs 2 and 3 are research laboratories.

Labs 2 and 3 have tested on materials which have a completely identical grain size distribution and have performed the tests according to the exact same procedures. But even these small differences in the boundary densities (1–2% on density) have a disproportionate effect on the calculated D_r: a void ratio e of 1.2 is equivalent to a D_r of 61% for lab 2, and 54.7% for lab 3.

3. Calibration chamber testing

Calibration chamber testing allows us to establish correlations between the CPT cone resistance q_c and other soil

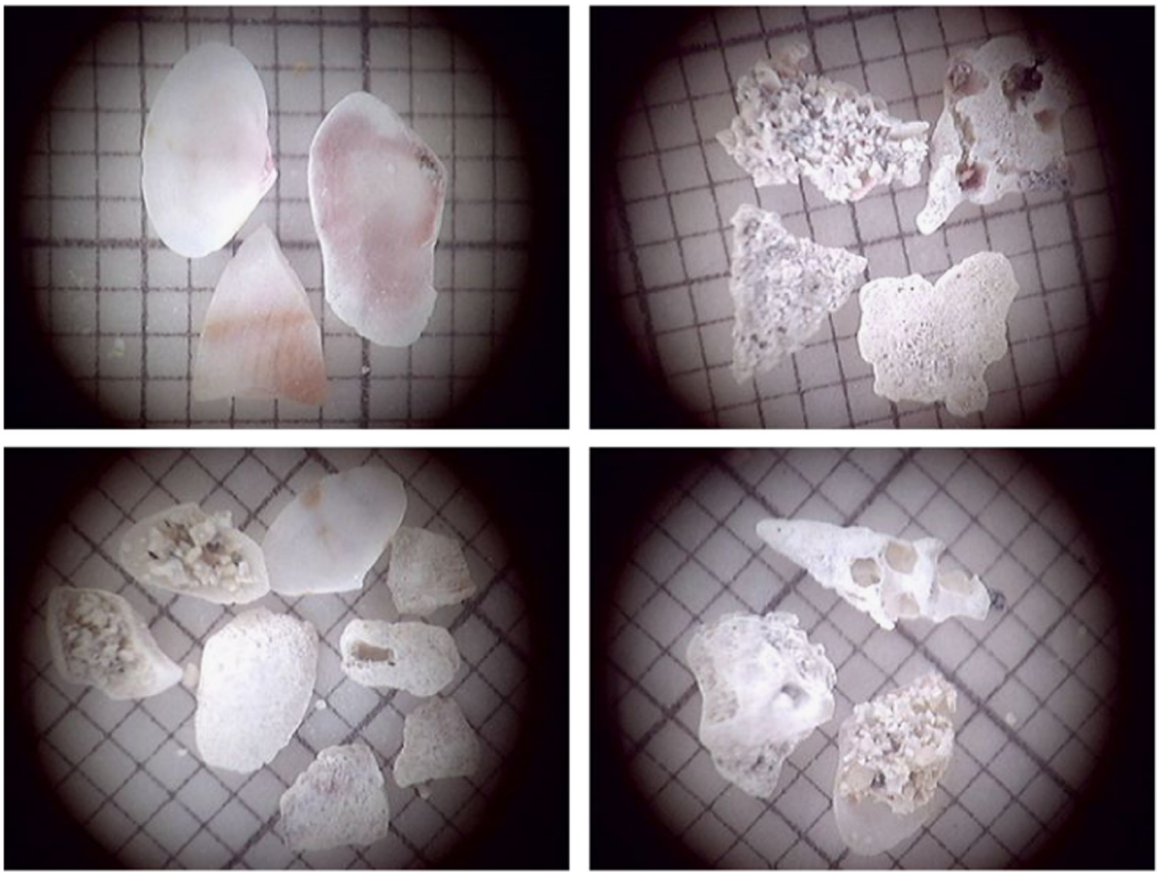

Fig. 2. Typical grain morphology of S1 sand.

Table 2
Variation in index densities on BAE samples.

Lab	Origin	Min. density[a] (kN/m^3)	Max. density[b] (kN/m^3)
Lab 1	BAE batch 1	12.56*	13.77
Lab 1	BAE batch 2	12.56*	15.11
Lab 2	BAE batch 3	10.92	14.08
Lab 3	BAE batch 3	11.20	14.20

[a]Min density D4254 method A (funnel).
[b]Max density D4253 (vibratory table).
*Except * D4254 method C (graduated cylinder).

parameters, in this case void ratio e (or relative density D_r) and the (vertical) effective stress level σ_v'.

3.1. Testing equipment and method

The calibration chamber tests have been performed in a centrifuge. This has the main advantage that q_c–D_r relations can be established at a continuous range of overburden pressures, while the traditional calibration chamber test only results in a single q_c–D_r–σ_v' data point for each test.

The ISMGEO geotechnical centrifuge, located at the former ISMES Geotechnical Institute in Bergamo, Italy, is a medium sized beam centrifuge with a symmetric rotating arm that holds two swinging baskets, containing the model and the counterweight. It has a capacity of 240 g-ton, designed to reach a limiting speed of 600 g with a payload of 400 kg. As we were interested in the overburden stress range from 50 to about 250 kPa, the tests have been performed at an acceleration level of 50g.

The calibration chamber is a cylindrical strong box with a diameter of 400 mm. The sample height inside this chamber is also about 400 mm.

The cone penetrometer is mounted on top of the cylindrical box. The miniature cone has a diameter of 11.3 mm and a total area of 100 mm^2. It has a 60° cone tip with a load cell to measure tip forces up to 9.8 kN and a 370 mm long shaft (diameter 11 mm) which connects to an upper section that contains a 9.8 kN load cell to measure cone shaft friction. The cone also has a pore-water-pressure transducer for interstitial pressure measurements.

The calibration chamber diameter ratio for the miniature cone is just above 35. Based on the general findings in literature for silica sands, we can assume that no boundary effects will occur, even less so because we are dealing with a crushable material.

The sample was reconstituted by pluvial deposition in air with a constant height of fall. To allow this, the material has been oven-dried and pre-sieved to 4 mm in order to avoid blockage of the pluviation system. The mass of the particle fraction larger than 4 mm is limited for both materials (less than 0.1% for BAE and 1.5% for BAW).

For each material, the pluviation system is calibrated to determine the fall height, the size of the hopper and the speed of the hopper to reach a specific density. Based on this correlation, the pluviation procedure can be adapted to reach the wanted densities. Samples have been tested with relative densities of approximately 40%, 60% and 70%.

During the acceleration, the sample was compressed. The consequent change in density was taken into account when analysing the results. The final density was based on the actual sample size after the required acceleration level has been reached (but before the cone penetration is performed). The method presented above has been proven its validity on many occasions (Lee, 1990; Bolton et al., 1999; Lee et al., 1999).

3.2. Results

Centrifuge calibration chamber tests have been performed on the BAE and BAW samples, both in dry and wet conditions. Fig. 3 shows the results of the tests on the BAW material using distilled water for the wet tests.

Jamiolkowski et al. (2001) in 2001 have proposed following form of the q_c–D_r–σ_v' correlation:

$$\frac{q_c}{p_a} = \exp(D_r \cdot C_2) \cdot C_0 \cdot \left(\frac{\sigma_v'}{p_a}\right)^{C_1} \quad (1)$$

where p_a is the atmospheric pressure in the same unit system of stress and penetration resistance (in our case p_a=98.1 kPa). C_0, C_1 and C_2 are non-dimensional empirical correlation factors. In the case of tests on Ticino (TS), Hokksund (HS) and Toyoura sand (TOS), following values for the correlation factors were suggested: C_0=17.68, C_1=0.50 and C_2=3.10.

The data obtained for the present case was analysed using the above correlation. The correlation factors for the BAE and BAW materials have been presented in Table 3, as are the values relevant for 'typical' silica sands (TS/TOS/HS).

Looking at these coefficients, there appears to be a significant impact of the presence of water, leading to much lower values of $q_{(c,wet)}$ as compared to $q_{(c,dry)}$ at similar relative density and stress level. However, eliminating the depth effect by using the normalized cone resistance Q_c, results of dry and wet tests are nearly identical. In order to unify the approach for wet and dry conditions, it could be preferable to reformulate the standard q_c–D_r–σ_v' correlations like (1) based on the normalized cone resistance Q_c:

$$Q_c = \frac{q_c - \sigma_v}{\sigma_v'} \quad (2)$$

where σ_v and σ_v' are the total and effective stresses, respectively.

It can also be noticed that although both the BAE and BAW sands have a clearly different particle size distributions they behave very similarly in the above mentioned calibration chamber tests. This indicates that the particle size distribution has less impact on the behaviour of the material than mineralogy and genesis.

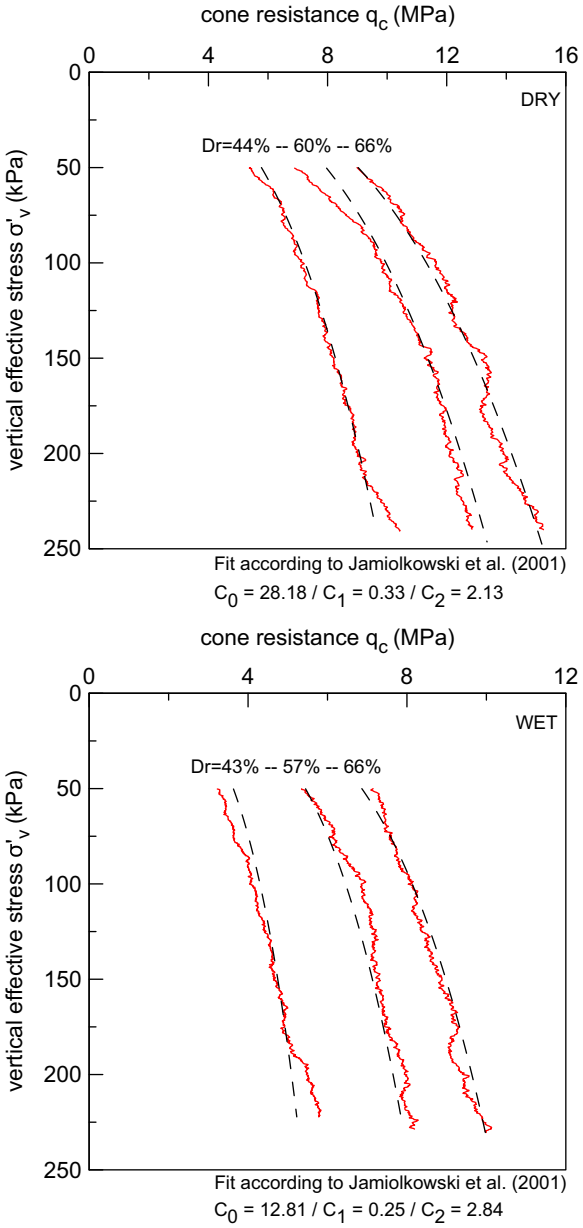

Fig. 3. Results of the laboratory centrifuge calibration chamber tests on BAW in both wet and dry conditions.

Table 3
Coefficients for q_c–D_r correlation.

Coeff.	BAE dry	BAE sat	BAW dry	BAW sat	TS+TOS+HS dry
C_0	22.64	13.09	28.18	12.81	17.68
C_1	0.42	0.29	0.33	0.25	0.50
C_2	2.40	2.68	2.13	2.84	3.10

An additional calibration chamber test was performed on the BAW sand using seawater as the testing fluid. Results were nearly identical to the test with distilled water, indicating that there was no effect of pore water chemistry on the results.

4. Triaxial and resonant column tests

In the second laboratory testing campaign tests have been performed on the S1 material which came from one of the actual reclamation sites. As mentioned above, the particle size distribution of this material was almost identical to that of the BAW sand.

As the main design decisions were linked to settlements the laboratory testing campaign focused mainly on determining stiffness parameters.

4.1. Overview and method

Nine drained triaxial tests (CD-TX) have been performed to analyse the stress–strain behaviour of the material over a large range of strain levels. To optimize the analysis of the stiffness of the sample, triaxial tests have been performed using local strain measurement devices. Bender elements (BE) allowed for measuring initial stiffness G_0 and M_0 during consolidation in the triaxial cell.

Additionally, two resonant column (RC) tests have been performed to evaluate stiffness decay and damping ratio for an isotropically consolidated saturated and dry sample.

Density, stress level and stress ratio have been varied. All samples were saturated and normally consolidated. Table 4 gives an overview of the tests.

The triaxial specimens had a height of 140 mm and a diameter of 70 mm. They were reconstituted by pluvial deposition in air of the dry sand. After saturation using CO_2 flushing, they were consolidated. In case of $K_0 = 2$, the sample was consolidated isotropically until $\sigma_v' = 200$ kPa, after which the vertical stress was kept constant and the radial stress increased in steps of 50 kPa, up to the final value.

At the end of each consolidation step, the velocity of seismic compression V_P and shear waves V_S has been measured using the bender elements (BE). This has allowed us to evaluate the initial small-strain stiffness.

At the end of consolidation, the samples were subjected to monotonic drained compression up to failure. (In the case of CD-TX 7 through 9, failure was obtained by keeping the horizontal stress constant and decreasing the vertical stress level.) During the shearing, local axial and radial strains were measured using proximity transducers in order to evaluate the stiffness decay.

Samples in the resonant column (RC) had a height of 100 mm and a diameter of 50 mm. The sample was isotropically consolidated in steps of 25 kPa. After each stage, the sample would undergo a small excitation which will allow us to determine the initial stiffness at this stress level. At the final stress level of 100 kPa, the full decay curve was determined, up to strain levels of about 0.1%.

Table 4
Overview triaxial and resonant column tests.

Test	K_0 (–)	σ_v' (kPa)	e (–)	D_r (%)
CD-TX 1	0.5	400	1.108	31.7
CD-TX 2	0.5	400	0.935	63.8
CD-TX 3	0.5	400	0.774	93.9
CD-TX 4	1	400	1.108	31.7
CD-TX 5	1	400	0.922	66.4
CD-TX 6	1	400	0.752	98.0
CD-TX 7	2	200	1.080	36.8
CD-TX 8	2	200	0.933	64.2
CD-TX 9	2	200	0.762	96.2
RC sat	1	25–50–75–100	0.967	57.9
RC dry	1	25–50–75–100	0.949	61.3

4.2. Results

4.2.1. Shear strength

Typical peak shear angles for the S1 material were about 45–50°, depending on relative density. This high shear angle is a result of the angularity of the carbonatic soil particles. The peak shear angle will drop at very large stress levels due to particle crushing, but this is well beyond the typical working stress levels at this site. The residual shear angle was about 40–42° which confirmed earlier test-results on the BAE/BAW materials.

4.2.2. Poisson ratio

Fig. 4 shows the variation of Poisson ratio ν derived from the local and global strain measurements, as a function of axial strain level. (Results are given for test 3 and test 6, other test results were very similar.) We can see that ν starts at values of about 0.3–0.4 at very small strain levels and then decreases to the typical value of 0.15–0.2 at strain levels between 0.1% and 1%. After this, the Poisson ratio again increases to 0.5, overshoots and comes back to 0.5 at critical state. This behaviour is consistent with data published on Quiou sand by Fioravante et al. (1994).

It can be noticed that the decay of the Poisson ratio is slower for the IC sample (sample 6).

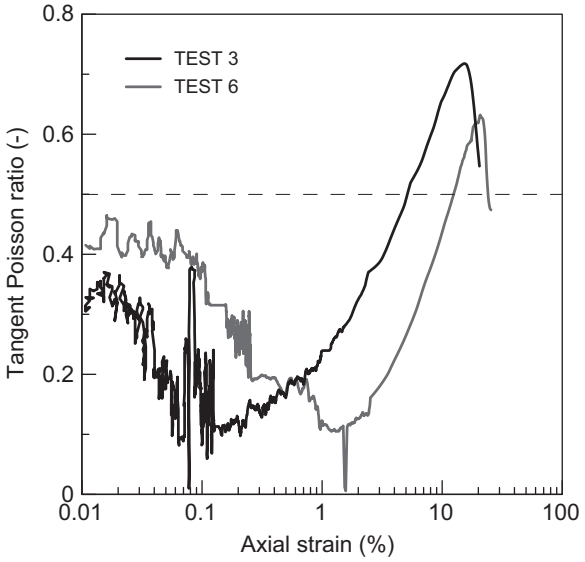

Fig. 4. Variation of the Poisson ratio in the TX test (based on local and global strain measurements).

At strain levels higher than 1%, local strain measurement devices were removed. From this level on, the Poisson ratio was based on global strain measurements. It can be seen that, at this strain level, there seems to be a good agreement between local and external measurements.

4.2.3. Small-strain stiffness from bender elements and resonant column test

The small-strain shear modulus G_0 is evaluated from the shear wave velocity V_s from bender element tests and the resonant column test on saturated samples.

Looking at the results in Fig. 5, there was a clear correlation between small strain shear modulus G_0, void ratio e and mean stress level p'. It was even possible to distinguish a slight impact of the anisotropic stress state. Based on the measurements, following correlations were proposed for the velocity of the shear wave V_S:

$$V_S = A_S \left(\frac{\sigma_v'}{p_a}\right)^{B_{Sv}} \left(\frac{\sigma_h'}{p_a}\right)^{C_{Sh}} e^{-D_S} \quad (3)$$

and the small-strain shear modulus G_0

$$G_0 = A_G \left(\frac{\sigma_v'}{p_a}\right)^{B_{Gv}} \left(\frac{\sigma_h'}{p_a}\right)^{C_{Gh}} e^{-D_G} \quad (4)$$

where p_a is the reference atmospheric pressure (98.1 kPa). The A, B, C and D parameters for each equation have been fitted to the data of the BE test in the laboratory triaxial equipment.

Fig. 6 represents the measured versus the predicted values of G_0, on the basis of the above mentioned correlation. The accuracy is quite good: for most points the deviation is less than 10%. The results of the dry RC test are outliers, indicating a slight impact of the presence of water on the results.

The small strain stiffness data was compared to the correlation proposed by Oztoprak and Bolton (2013) which is based on a very extensive database. Also some data from other authors has been added. Points lying on the main diagonal line represent data which agrees well with this correlation. Datapoints above this line would be underestimated using the correlation, while the opposite is true for the points below this line.

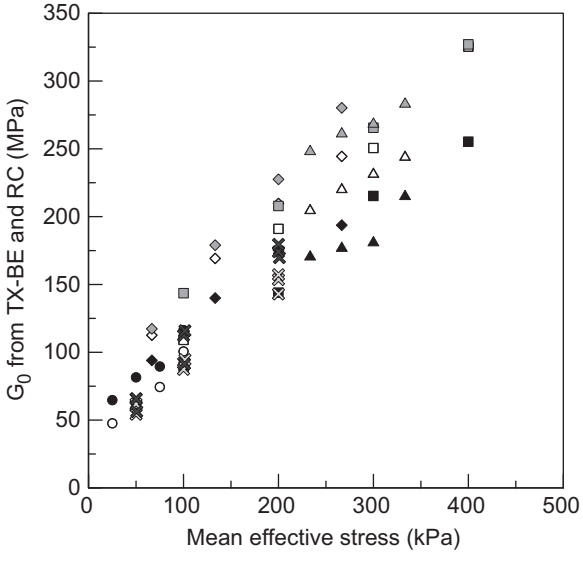

Fig. 5. Measured values of G_0 for S1/BAW/BAE sands at various void ratios as a function of mean effective stress level (own data from 9 TX and 2 RC).

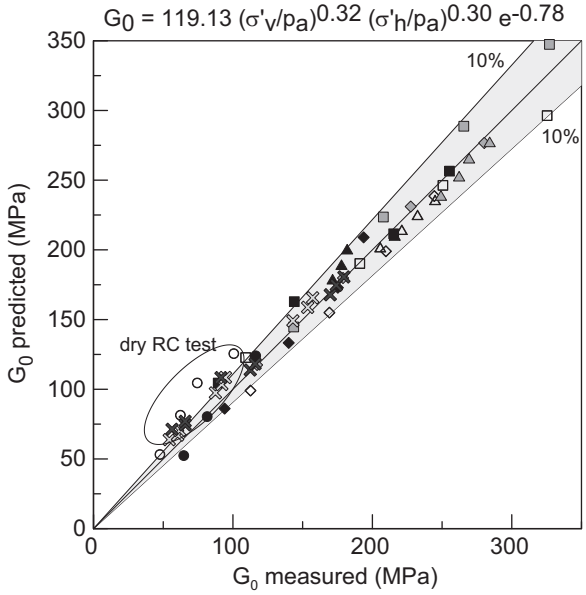

Fig. 6. Predicted versus measured value of G_0 S1/BAW/BAE sands (own data from 9 TX and 2 RC).

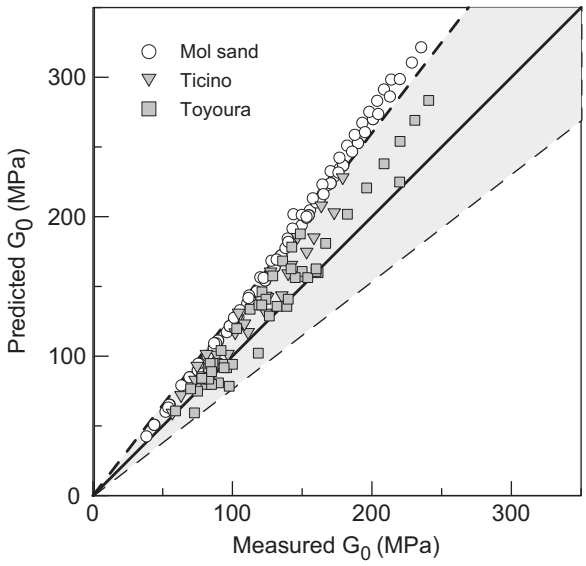

Fig. 7. Predicted versus measured G_0 for some silica sands (based on Oztoprak and Bolton, 2013.

Fig. 7 shows the data for Mol sand (Yoon, 1991), Ticino sand (Bellotti et al., 1996) and Toyoura sand (Iwasaki and Tatsuoka, 1977). It can be seen that all data points for these soils fall well inside the range of accuracy (about 30%) which was put forward by Oztoprak and Bolton in their 2013 paper.

Fig. 8 represents the data for calcareous sands like Quiou (Fioravante et al., 1994, 1998; Pallara et al., 1998), Dogs Bay (Jovicic and Coop, 1997), Cabo Rojo (Pando et al., 2012), Kenya (Fioravante et al., 2013) and the S1 sand from the present study. It can be noticed that the proposed correlation

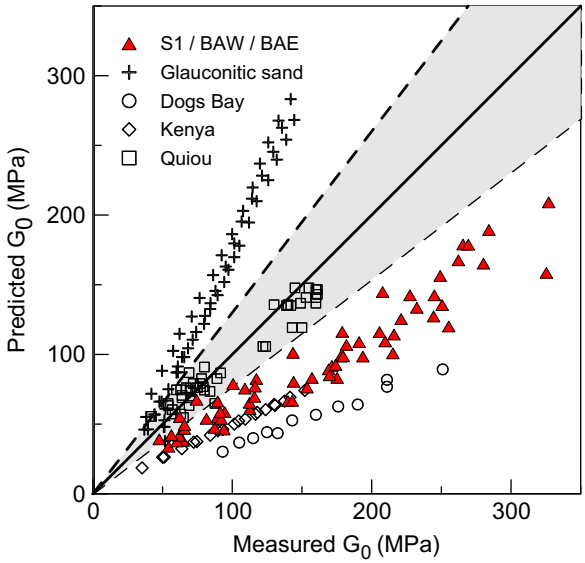

Fig. 8. Predicted versus measured G_0 for some calcareous sands (based on Oztoprak and Bolton, 2013).

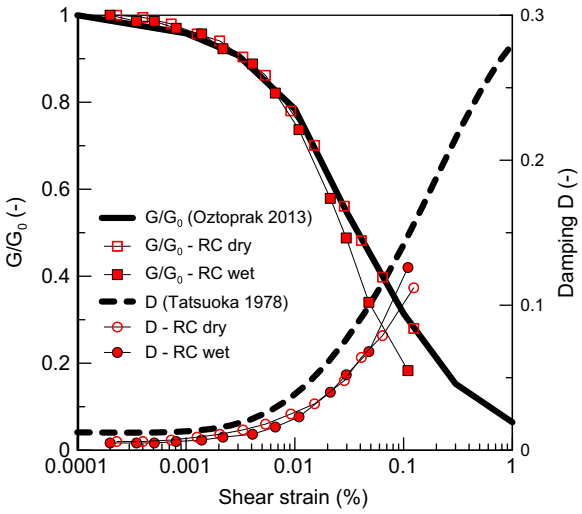

Fig. 9. Stiffness decay and damping for the S1 sands from RC.

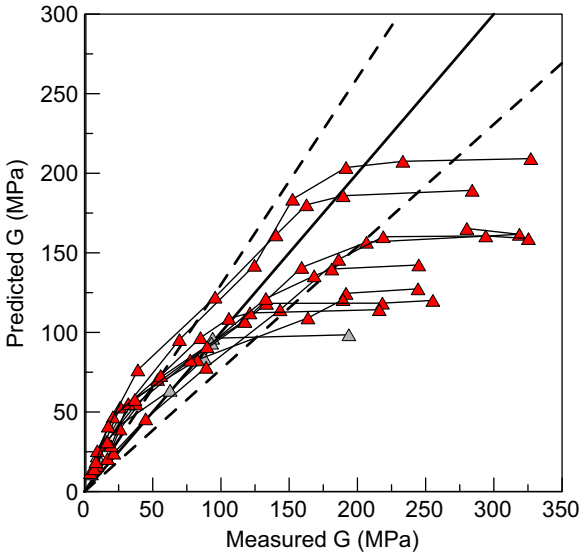

Fig. 10. Predicted versus measured G for the S1 sands from TX-CD (based on Oztoprak and Bolton, 2013).

(Oztoprak and Bolton, 2013) underestimates (significantly) the small strain stiffness of these materials. This is due to the fact that the range of void ratios for these materials is well beyond the typical range of void ratios for silica sands, as was clear from Table 1.

However, the data for most materials is still very much linear, indicating that the shape of the correlation (Oztoprak and Bolton, 2013) is still valid, and only has to be corrected with a different coefficient in order to make a better fit. One can conclude that for most sands – even for the more exotic ones like glauconitic sand (e.g. Antwerp sand, Yoon, 1991, see Fig. 8) – a reasonably reliable correlation between stress level, void ratio e and G_0 should exist.

From literature, it is known that the correlations can be adapted to take into account the effect of OCR. However, within the time frame of this project, we have only considered NC conditions.

4.2.4. *Stiffness decay*

Stiffness decay curves $G(\gamma)$ are available from the RC and TX tests. Fig. 9 presents the decay curve and damping coefficient of the S1 material in the RC test, for both wet and dry conditions.

The decay of the ratio G/G_0 for the wet material is steeper then what would be predicted by the correlation by Oztoprak and Bolton (2013). In dry conditions, we get a good fit. The damping coefficient for both tests is a bit lower that the prediction by Tatsuoka et al. (1978).

In absolute values however, the values of $G(\gamma)$ are still higher than those predicted by Oztoprak and Bolton (2013). As the degradation is faster, at some level of shear strain the absolute values will fall below the predicted values.

This is clear when looking at the results from the TX tests with the local strain measurements. These are presented in Fig. 10. In this graph, we compare each measured point at a specific strain level to the prediction using the correlation (Oztoprak and Bolton, 2013). The points move to the left, indicating a faster decay of stiffness. The fast decay compensates the high initial (small strain) stiffness. In fact, in this case, while the value of G_0 from bender elements would be about twice the predicted value, the stiffness at a strain level of 1% lies only at around 50–60% of the predicted stiffness at this strain level. This agrees with the findings in literature that crushable materials show a higher compressibility at working strains than 'typical' silica sands.

If we present our TX data in a more traditional way, relating the normalized Young modulus E_s/E_{max} to the shear strength mobilization q/q_f, we get Fig. 11. Clearly, the stiffness decay of the S1 sand during a triaxial test is significantly faster than the typical decay curve for NC silica sands, presented here using a modified hyperbolic curve (Fahey and Carter, 1993). We refer to Lo Presti et al. (1995), Fioravante et al. (1998) and Pallara et al. (1998) for similar graphs showing data on NC Toyoura and Quiou sand.

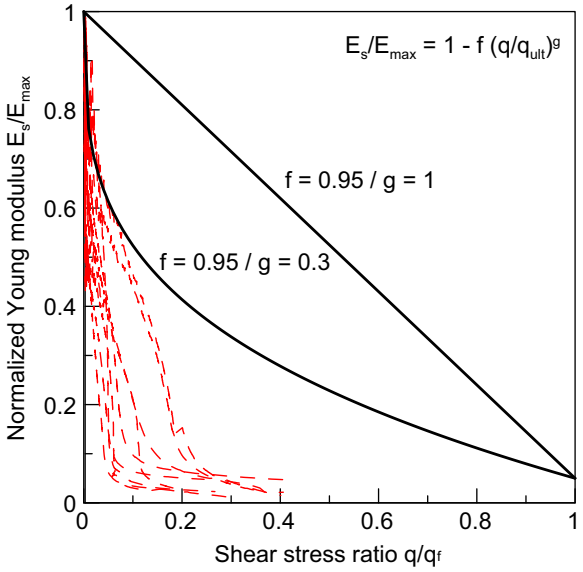

Fig. 11. Non-linearity of the S1 sand during triaxial tests.

The stiffness backbone curve is essential in design for translating in situ small strain stiffness data into working strain stiffnesses. A critical factor in the shape of this decay curve is the stress history. Fig. 12 presents results from literature on the decay curve for Quiou sand with different stress states and histories (Fioravante et al., 1994; Lo Presti et al., 1995; Pallara et al., 1998; Yamashita et al., 2000). The top figure is based on the comparison with the correlation (Oztoprak and Bolton, 2013), while the bottom figure gives the same data as a function of strain level. From this data, it is clear that stress history plays a major role in stiffness decay, in particular for calcareous sands.

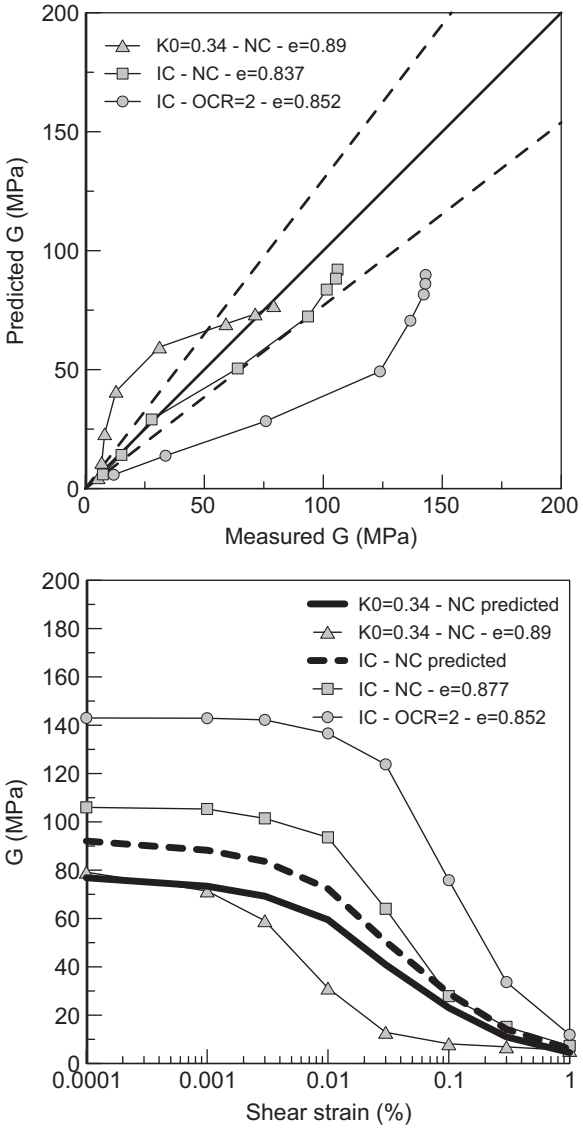

Fig. 12. Stiffness decay for Quiou sand samples with different stress states and stress histories.

4.2.5. *Small strain stiffness from CPT*

Several authors have proposed correlations between the CPT q_c and the small strain stiffness G_0.

The well-known graph in Fig. 13 presents the correlation between G_0/q_c versus the normalized cone resistance, proposed by Jamiolkowski and Robertson (1988) based on in situ data from NC and OC silica sands (Po river sand and Ticino sand). This was further expanded by Baldi et al. (1989) based on both laboratory and in situ testing.

Laboratory correlations are usually based on the determination of two separate elements: $qc = f(D_r, \sigma_v', K_0, OCR)$ and $G_0 = f(e, \sigma_v', K_0, OCR)$. Theoretically, assuming certain values for the state parameters, one could then find the corresponding value of the cone resistance q_c and the small strain shear modulus G_0. This procedure was used by Fioravante et al. (1991) on NC Toyoura sand data and by Fioravante et al. (1998) on NC and OC Quiou sand. From the latter data, it was clear that the original range presented by Jamiolkowski and Robertson (1988) would not fit data on a carbonatic sand like Quiou. Unlike silica sands, the G_0 over q_c ratio seems to be affected significantly by OCR for carbonatic sands.

Rix and Stokoe (1991) have widened this range to take into account a large number of data points, which were gathered for a range of soils, both in laboratory and in situ conditions. The graph 13 also contains our data points – based on the laboratory correlations which have been determined on the BAW and the S1 sand.

Although our laboratory data points fit reasonably well within the widened boundaries by Rix and Stokoe (1991), authors have some doubts on the validity of this approach in design:

- Representing data with the same variable in both axes (in this case q_c) *automatically* creates the impression of a correlation, a purely mathematical artefact. The graph in no way reflects an actual correlation between the main parameters G_0 and q_c.
- It should be clear that the actual range of values for G_0 in the above graph for a certain value of the (normalized) cone resistance is very large.

- Authors have generated values of G_0/q_c based on previously determined correlations. It can be seen from the graph that at a certain value of the (normalized) cone resistance, multiple values of the G_0 over q_c ratio exist. This is a result of the fact that the different combinations of the controlling parameters (D_r, σ_v', K_0, OCR) can lead to identical values of the cone resistance q_c but to different values of the small strain modulus G_0, or vice versa. Therefore, there can be no unique function linking q_c and G_0. This effect is limited in silica sands where stress anisotropy and OCR have little impact on either q_c and G_0. This is in our opinion absolutely not the case for calcareous materials.

The latter point has also been addressed by other researchers. Schneider et al. (2004) refers to the fact that 'since the number of controlling variables well exceeds the number of measured parameters, it is not possible to separate out the absolute role of each parameter'. Predicting the in situ G_0/q_c ratio may therefore require additional soil data to be available.

When compiling G_0 versus q_c data from sites with very different geotechnical characteristics (mineralogy, age, stress history, etc.), the boundaries in between which G_0 varies will lie well beyond those set by Rix and Stokoe (1991) (see Fig. 16 further on.)

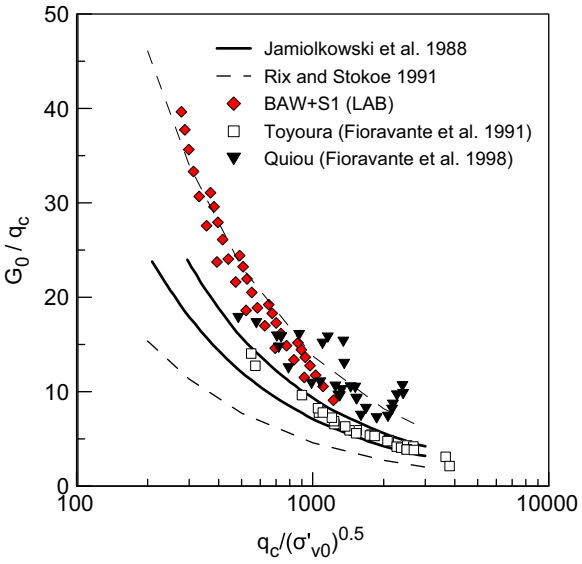

Fig. 13. Correlation G_0/q_c based on laboratory testing.

5. In situ testing

During the construction of the site, CPT was the main control test. Based on the cone resistance diagrams, profiles of relative density D_r were derived using the laboratory correlation. These profiles were then used to decide where and if compaction would be required. Compaction was continued until the required value of $D_r = 60\%$ had been reached.

After the vibrocompaction campaign, a series of 43 seismic CPTs (SCPT) were performed. These tests were analysed to determine D_r and G_0 from the laboratory correlations. Values of predicted G_0 were then compared to G_0 values measured during the seismic tests.

Figs. 14 and 15 show the analysis of two SCPTs. In the case of SCPT S1-26U, the test was done in an area where 2 vibrocompaction campaigns (VC) had been executed in order to reach the required relative density. In the area of SCPT S1-20W, only one compaction campaign was necessary. It can been seen from the analysis based on the laboratory correlation, that indeed the required value of relative density has been reached in both cases. The graph on the far right compares the predicted values of G_0 with the measured values. This graph also shows the prediction according to Robertson (2009) for young, uncemented silica sands.

The prediction is fairly accurate for SCPT S1-26U but really far from reality for SCPT S1-20W, although the CPT cone resistance profile for both cases is nearly identical below a level of 8–9 m, and although the energy input from vibrocompaction was higher in the first case.

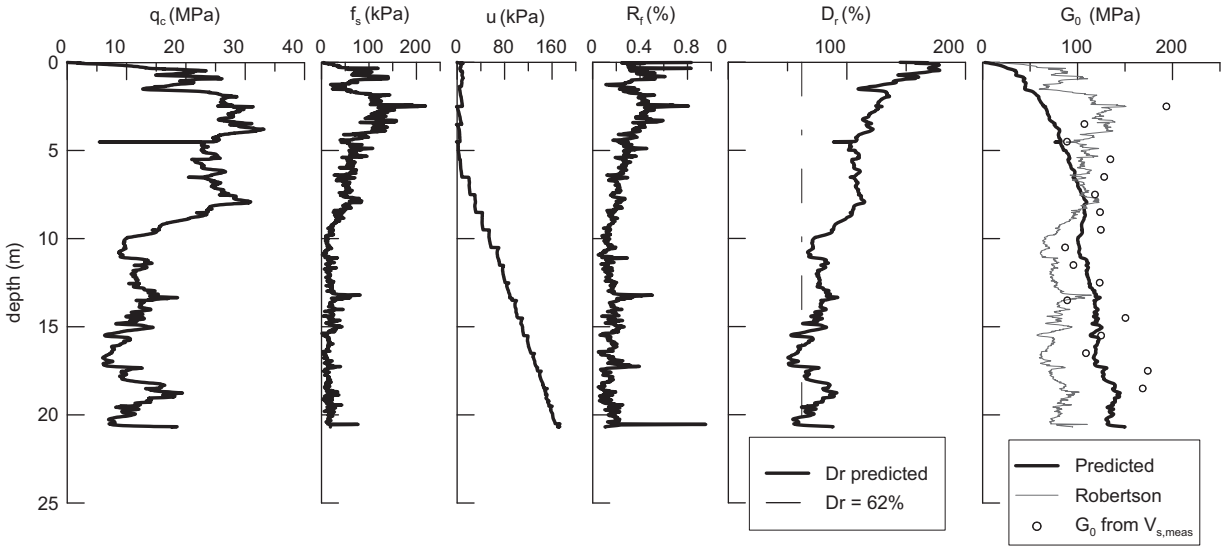

Fig. 14. Results of SCPT in area S1-26U performed after 2 VC campaigns. Determination of D_r and comparison between predicted G_0 and G_0 from measured V_S.

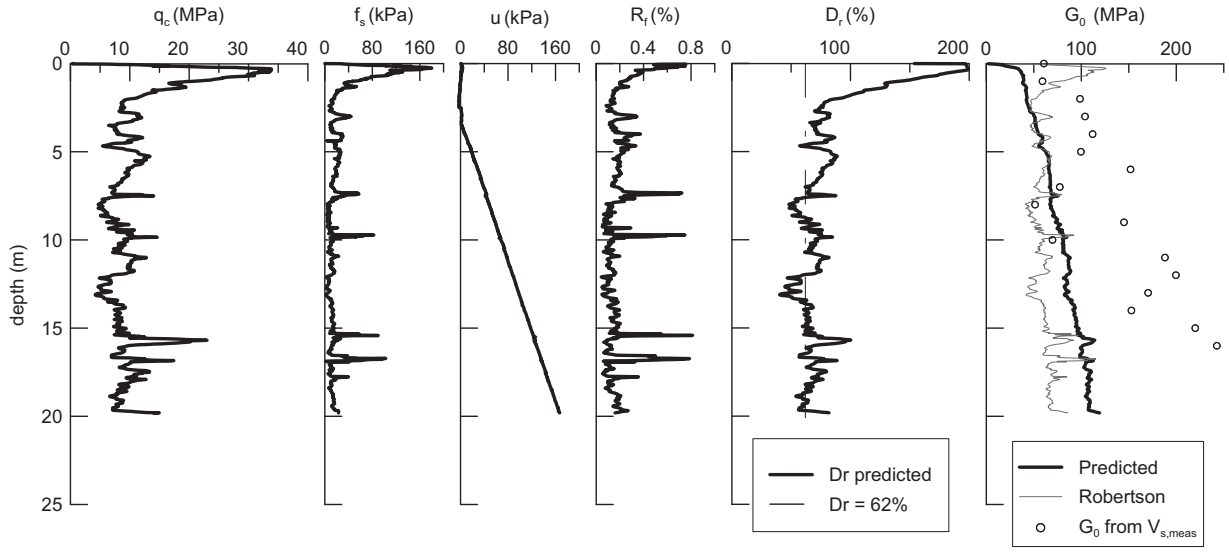

Fig. 15. Results of SCPT in area S1-20W performed after 1 VC campaign. Determination of D_r and comparison between predicted G_0 and G_0 from measured V_S.

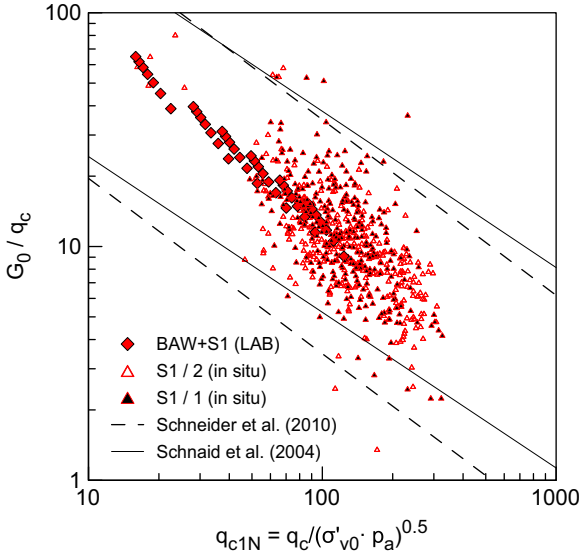

Fig. 16. G_0/q_c data from SCPT on both islands after VC campaign.

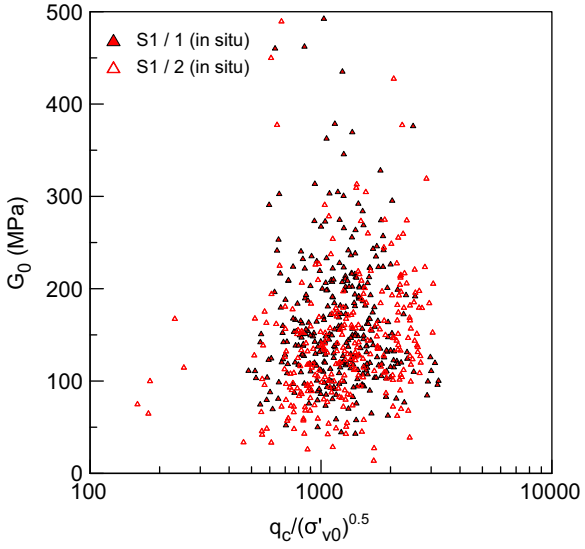

Fig. 17. Direct G_0 versus q_c data from SCPT on both islands after VC campaign.

These two cases were no exception. Compiling all SCPT data, we can draw the graph of G_0/q_c versus normalized cone resistance. This is illustrated in Fig. 16. Our data falls well within the boundaries as proposed by Schneider and Lehane (2010) (which are very similar to those proposed by Schnaid et al., 2004).

However, the actual range of G_0 values is enormous. This is clear from Fig. 17 which presents the values of the measured G_0 as a function of the normalized cone resistance, showing absolutely no correlation.

The data from the SCPTs has shown that the laboratory correlations do not allow a reliable prediction of the small strain modulus G_0 based on the results of a CPT.

It can also be noticed that the predicted value of the relative density D_r reaches beyond the maximum level of 100%. This is mainly due to the fact that the correlation between cone resistance q_c and relative density D_r is not valid at low stress levels, but could also be the result of extensive crushing of the top layer due to surface compaction.

Clearly, the laboratory correlations would need to include several other essential elements, like stress anisotropy and OCR, as they have a significant impact on the stress–strain behaviour (the small strain moduli and their strain-dependence), specifically in the case of crushable materials.

Extending the laboratory correlations to include these factors, at tremendous cost of time and money, however would not be the final answer. As put by Schneider et al. (2004), additional in situ soil information – like accurate measurements of the stress anisotropy and stress history – is required to be able to use these laboratory correlations. The CPT cannot, by itself, provide this information.

Moreover, in some conditions, the most influential factor would be the effect of crushing itself. This effect would significantly limit the relevance of the determined correlations. Most compaction techniques on site will inherently cause crushing on a large scale. In fact, in some situations, the densification criteria could be so strict that they can *only* be accomplished by inducing crushing in the soil.

6. Conclusions

The paper presents data of laboratory and in situ testing on a calcareous sand. Correlations were established between cone resistance q_c and relative density D_r and between the small strain shear modulus G_0, void ratio e and the stress level. These were combined to give a correlation between q_c and G_0.

The q_c–D_r correlation was used to determine the soil density on the site. Vibrocompaction was performed until a minimum value of $D_r = 62\%$ was obtained all over the site.

The q_c–G_0 correlation was used to predict the value of the small strain shear modulus G_0. SCPT tests were performed to validate these predictions.

The data presented here shows that although reasonable good correlations could be established in the laboratory, these correlations did not allow us to make a reliable prediction of the in situ soil behaviour, in this case small strain stiffness. In particular, it has been shown that there exists no direct correlation between cone resistance q_c and the small strain shear stiffness G_0 measured on the site.

This is due to several effects. Stress anisotropy and stress history have a significant impact on the behaviour of the calcareous material. These elements are especially very erratic in an off-shore land reclamation due to the methods of construction (dumping, rainbowing, etc.) and densification (vibrocompaction, heavy tamping, etc.). And while stress anisotropy and history are known or can be controlled in laboratory tests – and can therefore be taken into account when establishing the correlations – CPT testing does not provide enough data to determine these factors on site.

Additionally, laboratory correlations are determined using the original – unchanged – material. Extensive compaction efforts on the site will inevitably cause crushing in the soil material, in effect risking to render all laboratory correlations irrelevant. In many situations, crushing the soil material is the only way to meet certain density criteria. It is not always clear if the effect of crushing is beneficial to the behaviour of the material. Additional research is being done by the authors to investigate the impact of crushing on e.g. the liquefaction potential of calcareous sands.

In the case of the small strain stiffness G_0, the SCPT (seismic CPT) can provide a direct measurement and thus circumvent the above problems. The question remains if the same can be done for establishing e.g. the stiffness degradation (backbone curve) (Amoroso et al., 2013) or the liquefaction potential.

In this paper, authors have expressed their doubts about the principle of quality control for reclamations with calcareous sands based on the CPT. They propose contractors and designers to abandon the q_c–D_r approach in favour of a quality control philosophy directed towards actual relevant soil parameters. They believe that although laboratory testing is essential for the understanding of the basic soil behaviour, an increased effort should go towards the interpretation and development of in situ testing.

Acknowledgements

Authors wish to acknowledge Prof. Fioravante for his essential invaluable input and the high quality testing at ISMGEO.

Authors also wish to acknowledge the client ADMA-OPCO and COWI (the engineer) for their support in going 'beyond' the normal duties, in an effort to obtain valuable data regarding the behaviour of off-shore reclamations.

References

Amoroso, S., Monaco, P., Marchetti, D., 2013. Use of the seismic dilatometer (SDMT) to estimate in situ G–γ decay curves in various soil types. In: ISC4 on Geotechnical and Geophysical Site Characterization, pp. 489–497.

Baldi, G., Bellotti, R., Ghionna, V.N., Jamiolkowski, M., Lo Presti, D.C.F., 1989. Modulus of sands from CPT's and DMT's. In: 12th International Conference on Soil Mechanics and Foundation Engineering. Rio de Janeiro, Brazil, pp. 165–170.

Bellotti, R., Jamiolkowski, M., Lo Presti, D.C.F., O'Neill, D.A., 1996. Anisotropy of small strain stiffness in Ticino sand. Géotechnique 46 (1), 115–131.

Bolton, M.D., Gui, M., Garnier, J., Corte, J.F., Bagge, G., Laue, J., Renzi, R., 1999. Centrifuge cone penetration tests in sand. Géotechnique 49 (4), 543–552.

Brandes, H.G., 2011. Simple shear behavior of calcareous and quartz sands. Geotech. Geol. Eng. 29, 113–126.

Fahey, M., Carter, J.P., 1993. A finite element study of the pressure meter test in sand using a nonlinear elastic plastic model. Can. Geotech. J. 30 (2), 348–362.

Fioravante, V., 2000. Anisotropy of small strain stiffness of Ticino and Kenya sands from seismic wave propagation measured in triaxial testing. Soils Found. 40 (4), 129–142.

Fioravante, V., Ghionna, V.N., Jamiolkowski, M., Pedroni, S., 1998. Stiffness of carbonatic Quiou sand from CPT. In: Geotechnical Site Characterization, pp. 1039–1049.

Fioravante, V., Giretti, D., Jamiolkowski, M., 2013. Small strain stiffness of carbonate Kenya sand. Eng. Geol. 161 (July), 65–80.

Fioravante, V., Jamiolkowski, M., Lo Presti, D.C.F., 1994. Stiffness of carbonatic Quiou sand. In: 13th International Conference on Soil Mechanics and Foundation Engineering. New Delhi, pp. 163–167.

Fioravante, V., Jamiolkowski, M., Tanizawa, F., Tatsuoka, F., 1991. Results of CPT's in Toyoura quartz sand. In: 1st International Symposium on Calibration Chamber Testing. Potsdam, New York, pp. 135–146.

Hyodo, M., Hyde, A.F.L., Aramaki, N., 1998. Liquefaction of crushable soils. Géotechnique 48 (4), 527–543.

Iwasaki, T., Tatsuoka, F., 1977. Effects of grain size and grading on dynamic shear moduli of sands. Soils Found. 17 (3), 19–35.

Jamiolkowski, M., Ghionna, V.N., Lancellotta, R., Pasqualini E., 1988. New applications of penetration tests in design practice. In: 1st International Symposium on Penetration Testing, ISOPT-1. Orlando, Florida.

Jamiolkowski, M., Lo Presti, D.C.F., Manassero, M., 2001. Evaluation of relative density and shear strength of sands from CPT and DMT. ASCE Geotech. Spec. Publ. 119, 201–238.

Jamiolkowski, M., Robertson, P.K., 1988. Closing address. Future trends for penetration testing. In: Geotechnology Conference, Penetration Testing in the UK, Birmingham, United Kingdom, pp. 321–342.

Jovicic, V., Coop, M.R., 1997. Stiffness of coarse-grained soils at small strains. Géotechnique 47 (3), 545–561.

LaVielle, T.H., 2008. Liquefaction Susceptibility of Uncemented Calcareous Sands from Puerto Rico by Cyclic Triaxial Testing (Ph.D. thesis). Virginia Polytechnic Institute and State University.

Lee, K.M., Shen, C.K., Leung, D.H.K., Mitchell, J.K., 1999. Effects of placement method on geotechnical behaviour of hydraulic fill sands. J. Geotech. Geoenviron. Eng. 125 (October), 832–846.

Lee, S.Y., 1990. Centrifuge Modelling of Cone Penetration Testing in Cohesionless Soils (Ph.D. thesis). Cambridge University.

Lo Presti, D.C.F., Jamiolkowski, M., Pallara, O., Pisciotta, V., Ture, S., 1995. Stress dependence of sand stiffness. In: 3rd International Conference on Recent Advances in Geotechnical Earthquake Engineering and Soil Dynamics. St. Louis, Missouri, pp. 71–76.

Oztoprak, S., Bolton, M.D., 2013. Stiffness of sands through a laboratory test database. Géotechnique 63 (January (1)), 54–70.

Pallara, O., Lo Presti, D.C.F., Jamiolkowski, M., Pedroni, S., 1998. Caratteristiche di deformabilità di due sabbie da prove monotone e cicliche. Riv. Ital. Geotec, pp. 63–83.

Pando, M.A., Sandoval, E.A., Catano, J., 2012. Liquefaction susceptibility and dynamic properties of calcareous sands from Cabo Rojo, Puerto Rico. In: 15th World Conference on Earthquake Engineering. Lisbon.

Rix, G.J., Stokoe, K.H., 1991. Correlation of initial tangent modulus and cone penetration resistance. In: 1st International Symposium on Calibration Chamber Testing. Potsdam, New York, pp. 351–362.

Robertson, P.K., 2009. Interpretation of cone penetration tests—a unified approach. Can. Geotech. J. 46 (11), 1337–1355.

Schnaid, F., Lehane, B.M., Fahey, M., 2004. In situ test characterisation of unusual geomaterials. In: ISC2 on Geotechnical and Geophysical Site Characterization, pp. 49–73.

Schneider, J.A., Lehane, B.M., 2010. Evaluation of cone penetration test data from a calcareous dune sand. In: International Symposium on Cone Penetration Testing.

Schneider, J.A., McGillivray, A.V., Mayne, P.W., 2004. Evaluation of SCPTU intra-correlations at sand sites in the Lower Mississippi River Valley, USA. In: ISC2 on Geotechnical and Geophysical Site Characterization, pp. 1003–1010.

Tatsuoka, F., Iwasaki, T., Takagi, Y., 1978. Hysteretic damping of sand under cyclic loading and its relation to shear modulus. Soils Found. 18 (2), 25–40.

Yamashita, S., Jamiolkowski, M., Lo Presti, D.C.F., 2000. Stiffness non-linearity of three sands. J. Geotech. Geoenviron. Eng. 126 (October (1)), 929–938.

Yoon, Y.-W., 1991. Static and Dynamic Behaviour of Crushable and Non-Crushable Sands (Ph.D. thesis). Ghent University.

Further reading

Jamiolkowski, M., Ghionna, V.N., Lancellotta, R., Pasqualini E., 1988. New applications of penetration tests in design practice. In: 1st International Symposium on Penetration Testing, ISOPT-1. Orlando, Florida.